Multiple Secondary Structure Rearrangements during HIV-1 RNA Dimerization†

Hendrik Huthoff and Ben Berkhout*

Department of Human Retrovirology, Academic Medical Center, University of Amsterdam, Amsterdam, The Netherlands

Received April 22, 2002; Revised Manuscript Received June 11, 2002

ABSTRACT: HIV-1 RNA dimerization is a complex process that involves a series of RNA refolding events. The monomeric RNA can adopt two alternative conformations that largely determine the efficiency of dimerization. The dimeric RNA also exists in two different conformations, an initial kissing-loop complex and a stable dimer with extended intermolecular base pairing. We describe an ordered RNA folding pathway that incorporates this multitude of HIV-1 RNA conformers. Analysis of mutant transcripts designed to block distinct steps of the refolding cascade supports this model. The folding properties of the wild-type RNA and the defects caused by the mutations can be fully understood in terms of the free energy changes associated with secondary structure rearrangements.

Unspliced retroviral transcripts fulfill a dual role as mRNA and viral genome. Important regulatory RNA motifs for each of these functions are clustered within the untranslated leader RNA. The HIV-1[1] leader has a length of 335 nucleotides and contains RNA motifs involved in the regulation of transcriptional activation, splicing, polyadenylation, and translation but also RNA dimerization, genome packaging, and reverse transcription (Figure 1A) (*1*, *2*). In virus particles the retroviral genome is present as an RNA dimer that is noncovalently linked near the 5′ end (*3*, *4*). The RNA genome serves as a template for reverse transcription, and the dimeric state is thought to help bypass nicks or breaks during reverse transcription (*5*, *6*). It has also been suggested that the RNA dimer is preferentially packaged into virus particles (*7*, *8*).

We have recently demonstrated that the monomeric HIV-1 leader RNA can adopt alternative conformations (*9*, *10*). The thermodynamically favored conformation is an elongated fold in which remote domains of the leader are base paired through a *l*ong-*d*istance *i*nteraction (LDI) (Figure 1B). In the alternative conformation, the LDI is disrupted to allow folding of the *b*ranched *m*ultiple *h*airpin structure (BMH). The BMH conformer contains the *d*imer *i*nitiation *s*ite (DIS) hairpin, which is also referred to as *s*tem *l*oop 1 (SL1) or the *k*issing-*l*oop *d*omain (KLD). The DIS hairpin initiates RNA dimerization in vitro (*1*, *11*−*16*). The DIS hairpin is not present in the LDI structure, and this may provide the virus with a means to regulate RNA dimerization through a conformational switch between the LDI and BMH forms (*9*).

DIS-mediated RNA dimerization has been studied extensively using a variety of approaches, including NMR analyses (*17*−*20*), crystallography (*21*, *22*), and biochemical studies (*23*−*26*). Dimerization is initiated by base pairing of two loop-exposed palindromes, a structure referred to as the kissing-loop complex (KL, Figure 1B). After KL complex formation, the two DIS hairpin stems rearrange such that the intermolecular duplex is extended. This extended duplex dimer (ED, Figure 1B) is of higher thermal stability than the KL complex (*12*, *16*, *27*).

When taking into account the alternative monomeric RNA conformations (LDI and BMH) and the two different dimeric forms (KL and ED), dimerization becomes a complex process that requires multiple conformational rearrangements. We have constructed a hypothetical pathway to describe the steps required to convert LDI monomers into ED dimers (Figure 1B). This pathway includes the LDI and BMH monomeric conformations, the KL and ED dimers, and two putative folding intermediates, Int^A and Int^B. We tested the validity of this multistep RNA folding pathway with mutant transcripts. This model accurately predicts the dimerization properties of the wild-type transcript and the folding defects of mutant transcripts.

MATERIALS AND METHODS

In Vitro Transcription. RNA was transcribed from PCR-generated templates with a T7 promoter directly upstream of the transcriptional start site (position +1) of the HIV-1 LAI isolate. PCR was performed on the pBluescript 5′LTR plasmid (*28*) with a sense primer encoding the T7 promoter sequence and an antisense primer up to position 270 or 290. Mutant 270 + 4 was generated by introduction of four additional nucleotides in the antisense PCR primer. Construction of mutant GC1 has been described previously (*29*). PCR fragments were precipitated with ethanol and washed before use in transcription reactions. Transcription was performed with the Ambion megashortscript T7 transcription kit according to the manufacturer's instructions. Radiolabeled transcripts were synthesized in the presence of [α-^{32}P]UTP. Transcripts were excised from a 4% denaturing polyacrylamide gel (visualized by autoradiography) and eluted from the gel fragment by overnight incubation at room temperature in 0.3 M sodium acetate buffer (pH 5.2). The RNA was

† This work was supported by The Netherlands Organization for Scientific Research (NWO-CW).

* Corresponding author: tel, (31-20) 566 4822; fax, (31-20) 691 6531; e-mail, b.berkhout@amc.uva.nl.

[1] Abbreviations: HIV-1, human immunodeficiency virus type 1; NC, nucleocapsid protein; DIS, dimer initiation signal; LDI, long-distance interaction; BMH, branched multiple hairpin; KL, kissing-loop complex; ED, extended dimer; INT, intermediate.

10.1021/bi025993n CCC: $22.00
Published on Web 07/24/2002

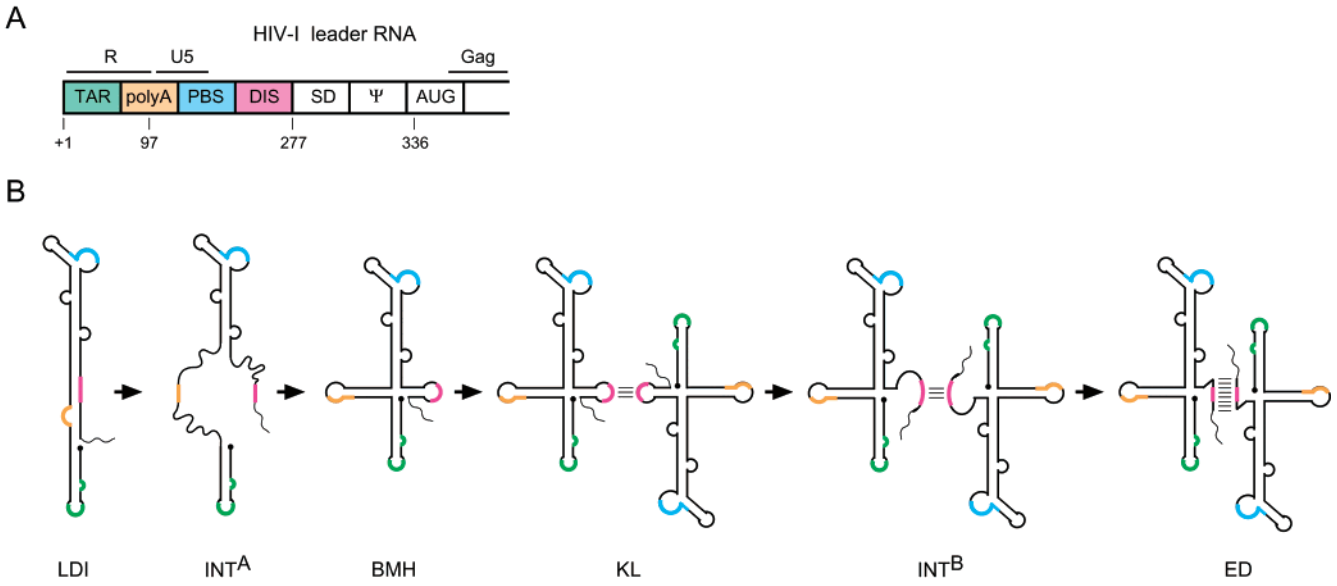

FIGURE 1: Structure and organization of the HIV-1 untranslated leader RNA. (A) Linear representation of the untranslated leader RNA, highlighting important regulatory motifs: TAR (trans-activation response element) in green, poly(A) (polyadenylation domain containing the AAUAAA sequence) in orange, PBS (primer binding site) in blue, DIS (dimerization initiation site) in pink, SD (major splice donor), ψ (core packaging signal), and AUG (the Gag start codon). (B) Schematic representation of the secondary structure conformations of the HIV-1 leader RNA. The thermodynamically most stable conformation of monomeric transcripts is an elongated rodlike fold, which is established through a long-distance interaction (LDI) between the poly(A) and DIS domains. After the poly(A) and DIS domains are dissociated (Int^A), the HIV-1 leader RNA rearranges into an alternative monomeric conformation: a branched structure containing multiple hairpins (BMH). Monomers in the BMH conformation can form dimers through intermolecular base pairing of the palindromic sequence that is exposed in the loop of the DIS hairpins: the kissing-loop complex (KL). The KL complex will remain associated through the palindromic sequence as the DIS stems dissociate (Int^B) to give rise to a more stable extended duplex dimer (ED).

precipitated and dissolved in water. Purified transcripts in water were heated at 85 °C and allowed to slowly cool to room temperature. Stock solutions of RNA were stored at −20 °C, and aliquots were taken for subsequent analysis. Quantification of the RNA was done by scintillation counting of radiolabeled transcripts.

In Vitro RNA Dimerization and Nondenaturing Electrophoresis. For the analysis of dimer formation approximately 0.5 μg of RNA was diluted to a final volume of 10 μL of incubation buffer. Buffers used were Tris buffer (10 mM Tris-HCl, pH 7.5), TEN buffer (100 mM NaCl, 1 mM EDTA, 10 mM Tris-HCl, pH 7.5), and dimerization buffer (40 mM NaCl, 0.1 mM $MgCl_2$, 10 mM Tris-HCl, pH 7.5). The RNA was heated to 60 °C and slowly cooled to room temperature. The heating temperature was varied in experiments addressing the temperature requirement for dimer formation. For determination of the thermal stability of dimers, a single bulk sample (100 μL) was incubated at 60 °C and split into 10 μL aliquots, which were subsequently diluted with 10 μL of water and heated for 10 min at the indicated temperatures. For RNA titration experiments an increasing amount of unlabeled RNA was added to the reaction mixture. After incubation, the samples were chilled on ice and diluted with 5 μL of loading buffer (30% glycerol with BFB dye). Heat denaturation of control samples was performed in formamide loading buffer (Ambion) by heating at 85 °C. Samples were analyzed on a 4% polyacrylamide gel either in 0.25 × TBE (22.5 mM boric acid, 0.625 mM EDTA, 22.5 mM Tris-HCl, pH 8.0) or in 0.25 × TBM (22.5 mM boric acid, 0.1 mM $MgCl_2$, 22.5 mM Tris-HCl, pH 8.0). Native gels were run at room temperature for approximately 3 h at 150 V. Gels were dried and visualized by autoradiography. RNA bands were quantitated on a Storm 860 phosphorimager.

Secondary Structure Prediction and Free Energy Calculations. Calculation of the free energy values of HIV-1 RNA structures was performed with the Mfold 3.0 algorithm offered by the MBCMR Mfold server (http://mfold.burnet.edu.au/) (*30*−*32*). Standard settings were used, corresponding to 1 M NaCl at 37 °C, with a 5% suboptimality range. A single Mfold calculation produces a set of structures with the corresponding free energy values, thus yielding the data for the alternative LDI and BMH conformations of monomeric HIV-1 RNA. Free energy values for the intermediate structures with unpaired regions were obtained from the base pairing constraints of the Mfold program. The free energy of the kissing-loop interaction was set at −15 kcal/mol, which corresponds to a helix of six G-C base pairs (*24*). The kissing-loop energy for mutant GC1 is −5 kcal/mol. The energy value for the ED dimer was approximated by Mfold analysis of a model transcript with a duplicated DIS sequence, interrupted by a loop consisting of five adenosines. The energy penalty for this loop was subtracted from the calculated free energy value. This ED free energy was added to the free energy of the remainder of the transcript. Energy values of monomeric conformations were multiplied by two for comparison with dimeric structures.

RESULTS

HIV-1 RNA Mutants That Affect Distinct Steps of the LDI−*BMH*−*KL*−*ED Pathway.* To critically test the proposed pathway of structural rearrangements in HIV-1 RNA (Figure 1), we made mutant transcripts (Figure 2A) that were designed to block a specific step in the pathway. We performed computer-assisted secondary RNA structure analysis (see Materials and Methods) with the wild-type and mutant sequences to provide a first approximation of the

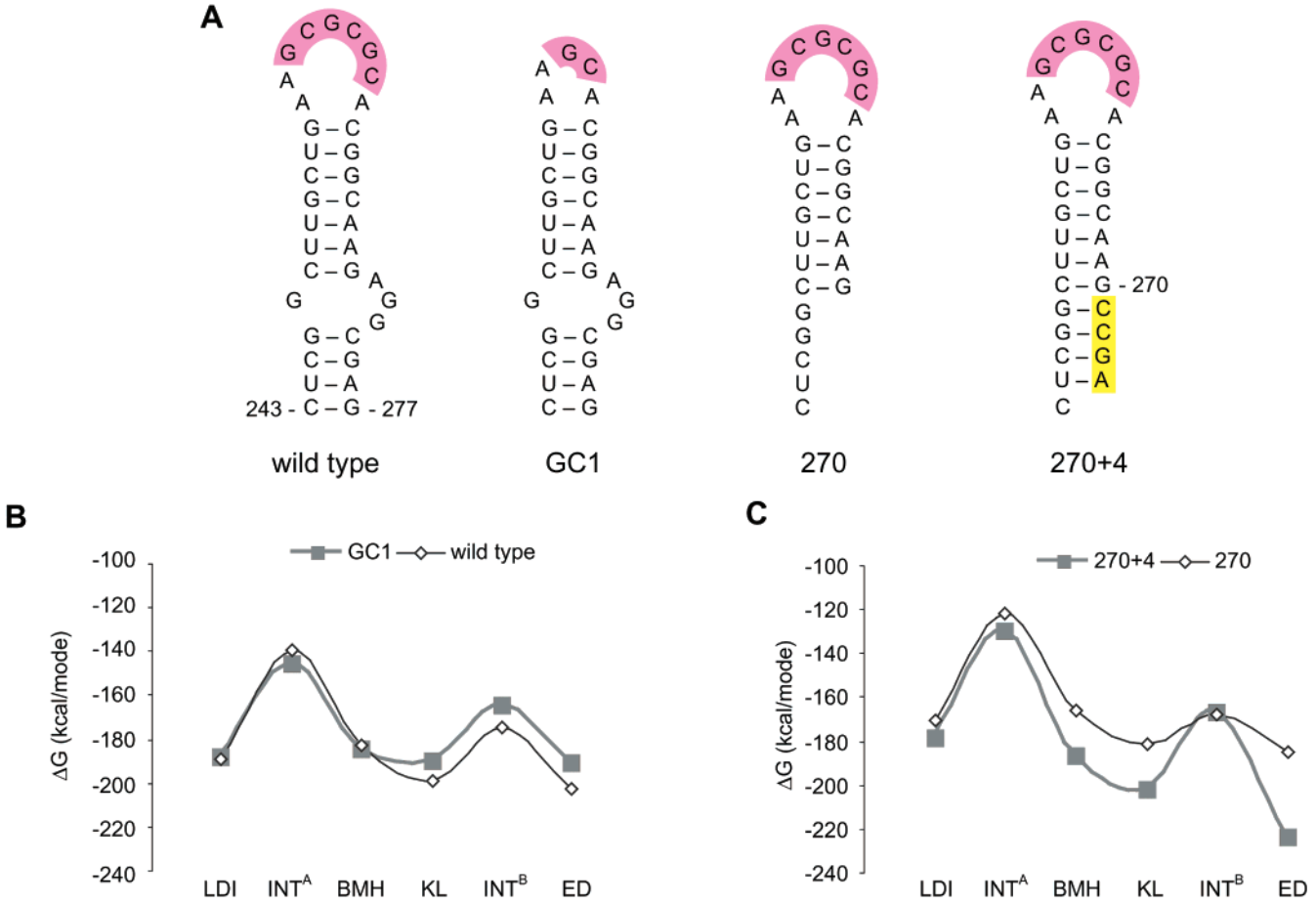

FIGURE 2: Wild-type and mutant DIS elements used in this study. (A) Mutant GC1 represents a deletion in the DIS palindromic sequence such that the wild-type GCGCGC sequence is reduced to GC. The DIS hairpin in transcripts 1/270 and 1/270 + 4 is also shown. The 270 + 4 mutant contains a 3′-terminal extension of four nucleotides at position 270 (highlighted in yellow), such that the DIS stem contains four additional base pairs. (B and C) Calculated free energy changes during HIV-1 RNA dimerization. Free energy values were calculated for all structures during the folding cascade as shown in Figure 1B. These conformations are indicated by abbreviations (see the text). We compared the GC1 mutant (B) and the 1/270 + 4 mutant (C) with the control wild-type sequence.

structural effects. The calculated free energy values (ΔG in kilocalories per mole) of the different RNA conformations were plotted for the wild-type and the mutant RNA (Figure 2B,C). The free energy plot of the wild-type transcript illustrates that the LDI is slightly more stable than the BMH. An energy barrier corresponding to the putative folding intermediate Int^A separates these two conformations. Part of the extended LDI stem is opened in Int^A to facilitate subsequent folding of the poly(A) and DIS hairpins in the BMH conformation. KL dimer formation reduces the free energy of the BMH molecule through the formation of six intermolecular G-C base pairs. Subsequent KL−ED isomerization generates the most stable leader RNA conformation. We included an unfavorable folding intermediate, Int^B, in which the DIS stems are melted to allow extension of the intermolecular base pairing interaction. In fact, this intermediate has been observed by NMR (*20*).

Mutant GC1 carries a four-nucleotide deletion in the DIS palindrome and was designed to block KL formation (Figure 2A). The free energy plot of this mutant indicates that the monomeric leader RNA conformations are affected only marginally by the deletion (Figure 2B). As expected, a significant drop in the stability of the KL is apparent, and this base pairing defect is maintained in the subsequent dimer structures (Int^B and ED). On the basis of this theoretical analysis, a selective RNA dimerization defect is expected for this mutant GC1.

Mutant 270 + 4 stabilizes the DIS hairpin by means of four additional bases that extend the stem with a perfect duplex downstream of position 270. The free energy calculations for this mutant are compared to the transcript terminating at position 270, which folds a truncated DIS hairpin that lacks the internal loop and lower stem (Figure 2A). The 270 + 4 mutation shifts the LDI−BMH equilibrium in favor of the BMH structure, which may increase dimerization through constitutive exposure of the DIS hairpin (Figure 2C). Stabilization of the DIS hairpin exerts additional effects; it increases the energy barrier for the KL−Int^B−ED transition because four additional base pairs need to be melted in each DIS hairpin. Thus, mutant 270 + 4 is predicted to form ED dimers poorly, but these ED dimers will be significantly more stable than the wild-type counterpart because of the eight additional intermolecular base pairs.

Mutation of the DIS Palindrome Exclusively Affects KL Dimer Formation. We first investigated the effect of disrupting the DIS palindromic sequence on the different conformations of the HIV-1 leader RNA. The LDI−BMH equilibrium and RNA dimerization were analyzed with the wild-type and mutant GC1 transcripts on a nondenaturing gel without Mg^{2+} (Figure 3). The transcripts were renatured in a buffer without

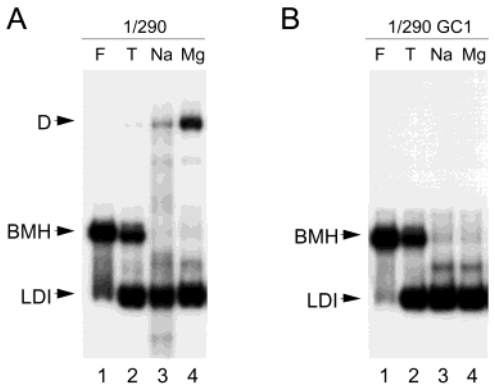

FIGURE 3: Dimerization assay with the wild-type and mutant GC1 transcripts at various ionic conditions. Conditions tested correspond to heat denaturation in formamide (F), 10 mM Tris-HCl buffer, pH 7.5 (T), 100 mM Na^+ (Na), and 40 mM Na^+ and 0.1 mM Mg^{2+} (Mg). Bands corresponding to the LDI, BMH, and dimer (D) conformations are indicated by arrows.

counterions (lane 2), a buffer with Na^+ (lane 3), and a buffer with Na^+ and Mg^{2+} (lane 4). As a control, formamide-treated samples have been included (lane 1). Both the wild-type and GC1 transcript adopt the fast-migrating LDI conformation on this nondenaturing gel. In the absence of counterions, the LDI and BMH conformations are in equilibrium for both transcripts (lane 2). Furthermore, both transcripts adopt the LDI conformation in the presence of cations (lanes 3 and 4). Thus, the LDI−BMH equilibrium is not detectably shifted in mutant GC1, which is in agreement with the predicted free energy (Figure 2B).

The wild-type transcript produces a low amount of RNA dimers in the presence of Na^+, and inclusion of Mg^{2+} strongly stimulates dimer formation (Figure 3A, lanes 3 and 4). Dimers of the GC1 mutant are not detectable, indicating that the DIS palindrome is important for KL dimer formation. Analysis of these RNA samples on a gel with Mg^{2+}, which stabilizes KL-type dimers, confirmed that the GC1 mutant is dimerization-impaired (results not shown). Nevertheless, this same mutant was previously shown to form RNA dimers in vivo (*29*). We therefore sought to identify conditions that support dimerization of the GC1 mutant. First, we made GC1 transcripts with a 5′-truncation of the TAR hairpin (17/290), which triggers BMH folding and a concomitant increase of the dimerization efficiency (*10*). Second, we generated conditions that favor formation of the KL dimer, such as high RNA concentration and high ionic strength (*20*, *33*). At low ionic strength, dimerization of the GC1 transcripts 1/290 and 17/290 is undetectable at all RNA concentrations (Figure 4A, lanes 2−5 and 7−10). A wild-type transcript was included as a positive control (lane 1), demonstrating increased RNA dimerization upon truncation of TAR (lane 6). Most importantly, GC1 dimers are made by the 17/290 transcript at high ionic strength (Figure 4A, lanes 17−20). GC1 RNA dimerization is dependent on the RNA concentration, and 14% dimer is made at micromolar RNA concentration (Figure 4A, lane 20). In contrast, the wild-type transcript yields 85% dimers at nanomolar RNA concentrations. Thus, dimerization of the GC1 mutant is facilitated by simultaneously favoring the BMH fold and KL dimer formation. No difference in GC1 dimer levels was apparent on TBM versus TBE gels (results not shown), indicating the GC1 dimers are of the ED type. These combined results indicate that the GC1 RNA is restricted at the level of KL formation, but a low level of ED dimerization can occur.

Stabilization of the DIS Stem Blocks Formation of the ED Dimer. The 1/270 + 4 monomer is predicted to adopt the BMH structure because the DIS hairpin is stabilized (Figure 2B). This may favor KL dimer formation, but the energy plot also predicts a severe defect in ED dimer formation. KL to ED isomerization can be induced by heat treatment (*12*, *16*, *27*, *34*), and we therefore investigated the effect of temperature on dimerization of mutant 270 + 4. We analyzed the RNA on two gel types to distinguish between KL and ED dimers (*12*, *27*, *35*). TBM electrophoresis with Mg^{2+} in the gel and running buffer preserves the relatively instable KL complex. KL dimers dissociate on a TBE gel because EDTA sequesters the Mg^{2+} that is important for maintenance of the loop−loop interaction, and ED dimers will be detected exclusively. On the TBM gel, the 270 + 4 transcript produced more RNA dimers than the wild-type control (Figure 5A, lanes 2 and 9). Strikingly, the situation is reversed on the TBE gel, where the mutant RNA produces less dimers than the wild-type transcript (Figure 5B, lanes 2 and 9). The RNA signals were quantitated to calculate the dimerization efficiencies (Figure 5C for the TBM gel and Figure 5D for the TBE gel). The 270 + 4 mutant forms predominantly KL dimers and very little ED dimers, which is consistent with the free energy prediction (Figure 2B) and a previous in vitro analysis of a similar mutant (*26*). Furthermore, inspection of the monomeric RNA on the TBE gel confirms that this mutant prefers the BMH fold (Figure 5B).

We tested whether ED dimer formation of mutant 270 + 4 can be rescued by increasing temperature in the 20−70 °C range, which may facilitate melting of the stabilized DIS stem. Dimerization of the wild-type RNA is observed at 20 °C and reaches a maximum at 55 °C (Figure 5B), because the dimer melts at higher temperatures. Interestingly, the mutant RNA requires temperatures above 50 °C for the formation of ED dimers (Figure 5B,D). This is consistent with the predicted increase in the energy barrier corresponding to the Int^B intermediate. In addition, this mutant is predicted to form excessively stable ED dimers due to the eight additional intermolecular base pairs. Indeed, the mutant dimers show no significant dissociation at high temperatures (Figure 5B). We formally assessed the thermal stability of the ED dimers in a melting experiment. A large RNA dimer sample was prepared, and aliquots were taken, diluted, and heated at varying temperatures (Figure 6). The wild-type ED dimers melt at 55 °C, which is consistent with previous results (*12*, *16*, *27*, *34*). The mutant ED dimers do resist temperatures up to 60 °C, which is in agreement with the predicted increase in stability caused by the additional intermolecular base pairs. Analysis of these samples on TBM gels indicated that the thermal stability of the KL dimer was not affected by the 270 + 4 mutation (results not shown).

DISCUSSION

We postulated an ordered pathway of RNA structure rearrangements to describe the complex mechanism of HIV-1 RNA dimerization. This RNA folding pathway includes the LDI and BMH conformations of the monomeric RNA, the KL and ED RNA dimers, and two folding intermediates

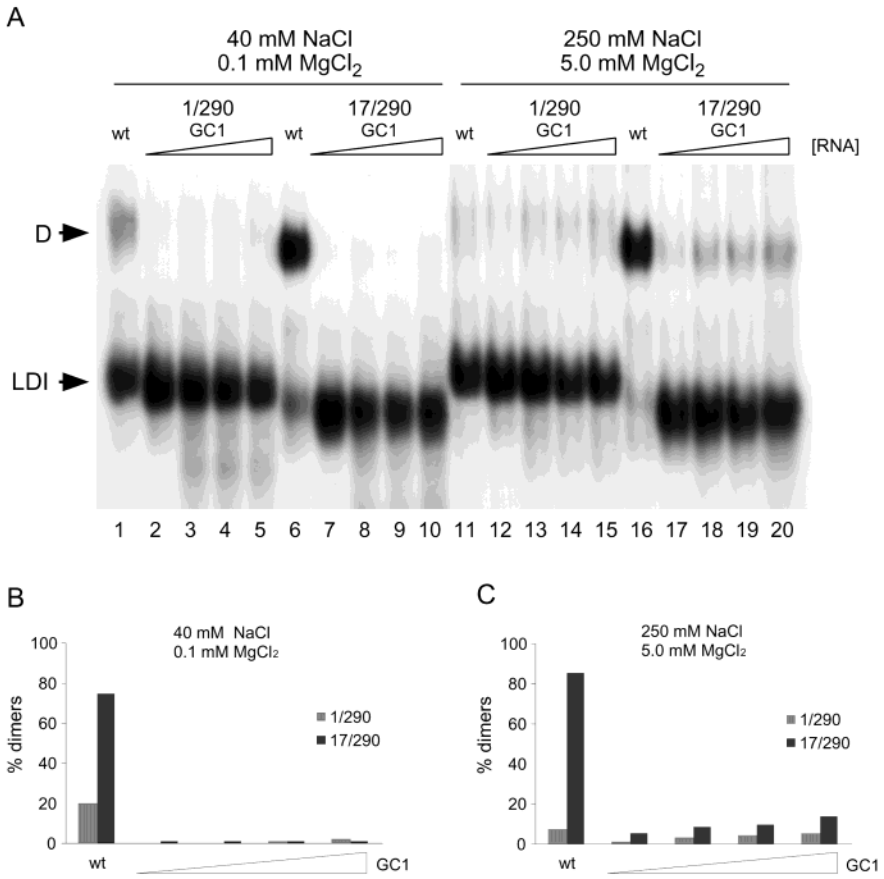

FIGURE 4: Dimerization of the wild-type and GC1 mutant RNA. (A) TBM gel showing a titration of the GC1 mutant in dimerization assays. Two different transcripts were used, 1/290 and 17/290, as indicated at the top of the lanes. Different ionic strengths were compared as indicated at the top of the gel. The GC1 RNA concentration was increased in the order 500 nM, 3.0 μM, 5.0 μM, and 10.0 μM. Wild-type control samples were tested at 500 nM RNA. Quantified data at 40 mM NaCl and 0.1 mM $MgCl_2$ (B) and at 250 mM NaCl and 5.0 mM $MgCl_2$ (C).

(Figure 1B). On the basis of this mechanism we predicted the free energy changes that occur during dimerization of HIV-1 RNA. We made mutant transcripts that are selectively blocked at a distinct step of this folding cascade.

Studies with the GC1 mutant showed that deletion of the DIS palindrome selectively affected dimerization. This mutant maintains a normal LDI−BMH equilibrium and folds a structure very similar to the wild-type LDI. The four-nucleotide deletion results in the loss of only two base pairs in the LDI stem because the wild-type LDI stem contains mismatched nucleotides (Figure 7). We recently demonstrated that the extended LDI stem can resist mutational attack (*36*). However, the same deletion has a relatively large effect on the stability, or the existence, of KL dimers because four of the six intermolecular base pairs are lost. Indeed, the free energy plot of the GC1 mutant first deviates from the wild type at the step of KL formation, and this dimerization defect was confirmed experimentally. Dimerization of mutant GC1 could be partially rescued by creating conditions that favor the formation of KL dimers, such as folding of the BMH structure and raising the RNA concentration and the ionic strength. It is also possible that these conditions induce ED dimerization from the BMH monomer via a monomeric Int^B-like structure to bypass the instable KL dimer of the GC1 mutant.

The results with the 270 + 4 mutant can also be explained by the predicted RNA secondary structure changes during dimerization. This mutant contains a stabilized DIS hairpin, which results in a preference for the BMH monomer. KL dimers are readily formed because dimerization is no longer restricted by the competing LDI structure. Indeed, KL dimerization of the 270 + 4 RNA exceeds the levels measured for the wild-type RNA that does adopt the LDI structure. However, the abundant pool of 270 + 4 KL dimers does not give rise to a corresponding amount of ED dimers. This can be explained by the increased energy that is required for melting of additional base pairs in the folding intermediate Int^B. The extreme thermal stability of ED dimers derived from the 270 + 4 RNA demonstrates that these additional base pairs participate in the intermolecular duplex.

The results of both mutants and the wild-type RNA support the notion that HIV-1 RNA dimerization can be understood in terms of the RNA secondary structure, that is, the melting and formation of base pairs. Nonetheless, a different RNA dimerization mechanism was recently proposed. On the basis of the KL crystal structure of the DIS hairpin, Ennifar et al. suggested that the KL to ED transition proceeds through autocatalysis (*22*). It was argued that the nucleotides directly flanking the DIS palindrome are favorably oriented for symmetrical cleavage and subsequent cross-religation to yield the ED dimer. However, if the nucleotides flanking the DIS palindrome form the catalytic core of a ribozyme, KL to ED isomerization should be insensitive to stabilization of the DIS stem. Our observation that the 270 + 4 mutant forms ED dimers poorly from an abundant pool of KL dimers challenges this autocatalytic mechanism. Furthermore, one would

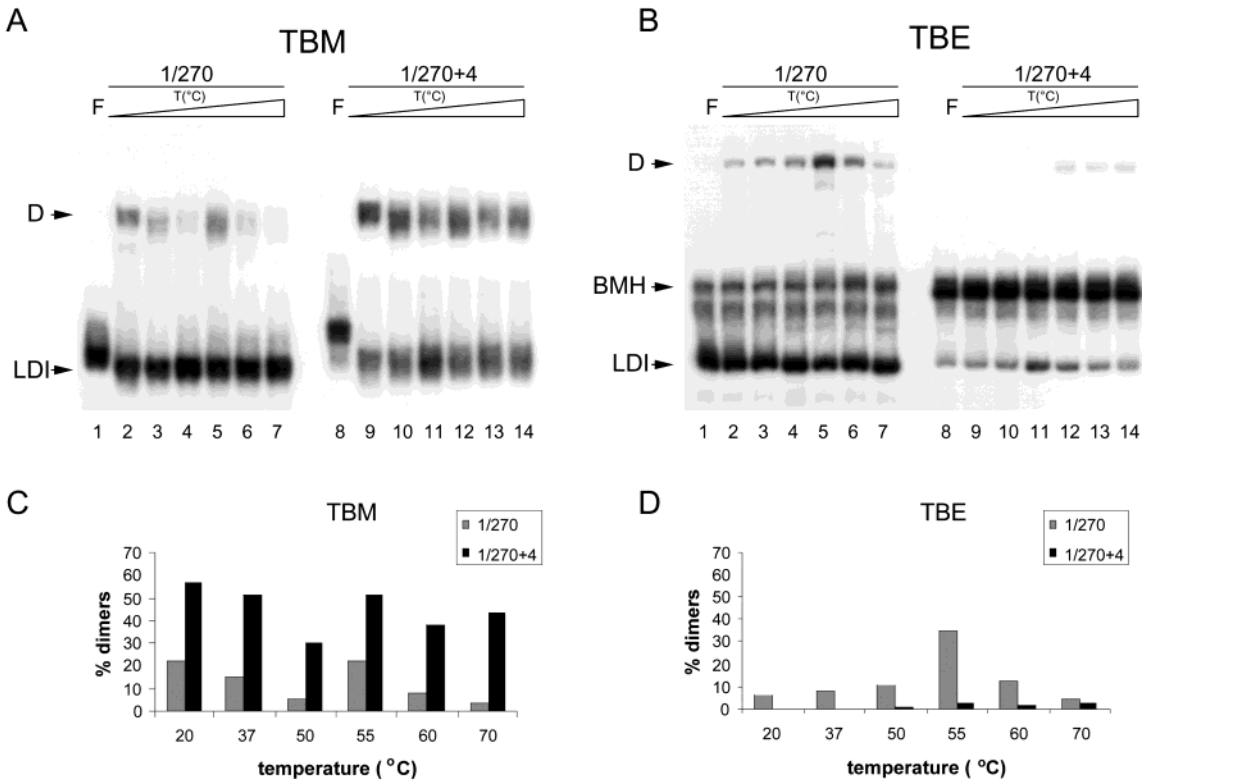

FIGURE 5: Temperature dependence of dimer formation by the wild-type 1/270 and mutant 1/270 + 4 transcripts. (A) Analysis on a TBM gel. (B) Analysis on a TBE gel. Formamide-denatured control samples have been included (F, lanes 1 and 8). Incubation temperatures correspond to 20 °C (lanes 2 and 9), 37 °C (lanes 3 and 10), 50 °C (lanes 4 and 11), 55 °C (lanes 5 and 12), 60 °C (lanes 6 and 13), and 70 °C (lanes 7 and 14). Bands corresponding to the LDI, BMH, and dimer (D) conformations are indicated by arrows. The 1/270 transcript is able to adopt the LDI conformation, and mutant 270 + 4 primarily produces the slow-migrating BMH conformation. (C and D) Quantified data from (A) and (B), respectively.

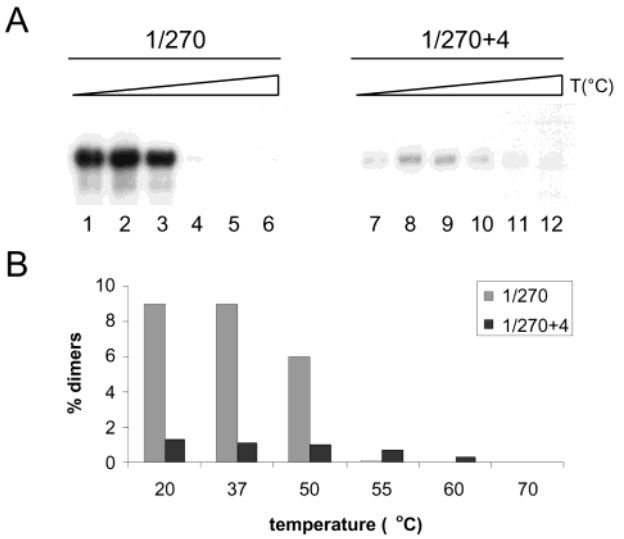

FIGURE 6: Thermal stability of the wild-type 1/270 and mutant 1/270 + 4 ED dimers. (A) Analysis of heat-treated dimers on a TBE gel. The RNA was incubated at 20 °C (lanes 1 and 7), 37 °C (lanes 2 and 8), 50 °C (lanes 3 and 9), 55 °C (lanes 4 and 10), 60 °C (lanes 5 and 11), and 70 °C (lanes 6 and 12). Only the dimeric bands are shown because the detection of the dimers from the mutant transcript required severe overexposure of the gel. (B) Quantified data from (A).

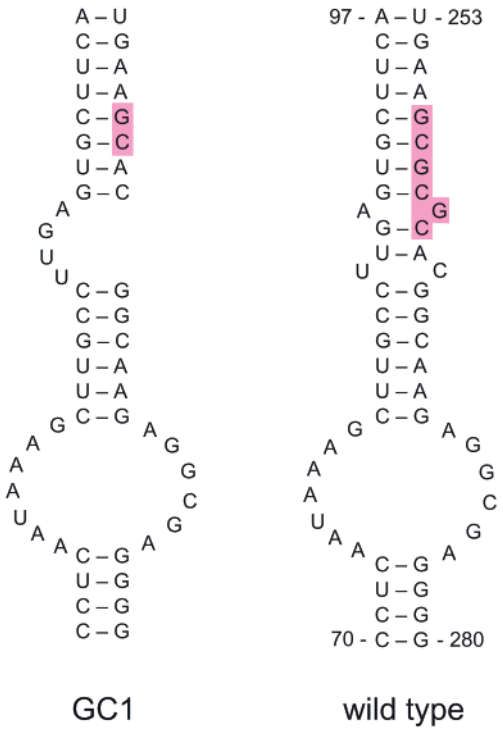

FIGURE 7: Predicted LDI structure of the GC1 mutant and the wild-type HIV-1 leader RNA. The DIS palindrome is highlighted in pink.

expect a cleavage−religation mechanism to produce reaction intermediates in vitro, but we did not detect such RNA species.

It has been difficult to reconcile the results of in vitro RNA dimerization assays with virus replication studies, suggesting that in vivo dimerization may differ in several aspects. For instance, the DIS palindrome mutant GC1 has a severe dimerization defect in vitro (this study), but the corresponding virions package a normal RNA dimer (*29*). Note, however,

that milder mutations in the DIS palindrome have been shown to substantially inhibit genome dimerization in isolated viruses (*37*). We demonstrated here that the in vitro dimerization defect of the GC1 mutant can be rescued with transcripts that prefer the BMH fold under conditions that favor dimerization (high RNA concentration and high ionic strength). It is possible that these conditions mimic the situation during virion assembly. In particular, there may be a high local RNA concentration in the virion. Furthermore, the viral nucleocapsid protein, NC, is abundantly present in virions and acts as a cofactor for RNA dimerization (*38*). NC has been shown to mediate the LDI to BMH switch (*9*) and the KL to ED rearrangement (*34*). In addition, the NC domain of Gag is important for selective recognition and packaging of the RNA genome. Several groups have reported that mutations that disrupt dimerization in vitro yield viruses with a packaging defect (*39*−*41*). In particular, the GC1 RNA is packaged with reduced efficiency (*29*). Likewise, mutants that stabilize the DIS stem similar to our 270 + 4 mutant exhibit RNA packaging defects (*40*) as well as dimerization defects in vivo (*42*). In contrast, recent studies demonstrated that duplication of the leader RNA at an ectopic position results in packaging of monomeric genomes without affecting the packaging efficiency (*43*, *44*). The interplay between genome dimerization and packaging thus remains an intriguing issue for future investigations.

We have shown that the HIV-1 leader RNA adopts a multitude of secondary structures during the process of genome dimerization in vitro. This dynamic model of the HIV-1 leader RNA may help to better understand the biological roles of this multifunctional RNA. The recent observation that the HIV-2 untranslated leader RNA also adopts alternative structures that modulate dimerization suggests that this may be a common feature in the replication strategies of the immune deficiency viruses and perhaps all retroviridae (*45*). RNA switches are of critical importance in other biological systems such as the regulation of mRNA translation (*46*−*50*) and the replication mechanism of viruses that exploit RNA intermediates (*51*−*53*).

ACKNOWLEDGMENT

We thank Wim van Est for the artwork.

REFERENCES

1. Berkhout, B. (1996) *Prog. Nucleic Acid Res. Mol. Biol. 54*, 1−34.
2. Berkhout, B. (2000) *Adv. Pharmacol. 48*, 29−73.
3. Bender, W., and Davidson, N. (1976) *Cell 7*, 595−607.
4. Hoglund, S., Ohagen, A., Goncalves, J., Panganiban, A. T., and Gabuzda, D. (1997) *Virology 233*, 271−279.
5. Hu, W.-S., and Temin, H. M. (1990) *Proc. Natl. Acad. Sci. U.S.A. 87*, 1556−1560.
6. Hu, W.-S., and Temin, H. M. (1990) *Science 250*, 1227−1233.
7. Darlix, J.-L., Gabus, C., Nugeyre, M. T., Clavel, F., and Barre-Sinoussi, F. (1990) *J. Mol. Biol. 216*, 689−699.
8. Fu, W., and Rein, A. (1993) *J. Virol. 67*, 5443−5449.
9. Huthoff, H., and Berkhout, B. (2001) *RNA 7*, 143−157.
10. Huthoff, H., and Berkhout, B. (2001) *Nucleic Acids Res. 29*, 2594−2600.
11. Laughrea, M., and Jette, L. (1994) *Biochemistry 33*, 13464−13474.
12. Laughrea, M., and Jette, L. (1996) *Biochemistry 35*, 1589−1598.
13. Skripkin, E., Paillart, J. C., Marquet, R., Ehresmann, B., and Ehresmann, C. (1994) *Proc. Natl. Acad. Sci. U.S.A. 91*, 4945−4949.
14. Paillart, J.-C., Skripkin, E., Ehresmann, B., Ehresmann, C., and Marquet, R. (1996) *Proc. Natl. Acad. Sci. U.S.A. 93*, 5572−5577.
15. Girard, P.-M., Bonnet-Mathoniere, B., Muriaux, D., and Paoletti, J. (1995) *Biochemistry 34*, 9785−9794.
16. Muriaux, D., Fosse, P., and Paoletti, J. (1996) *Biochemistry 35*, 5075−5082.
17. Mujeeb, A., Clever, J. L., Billeci, T. M., James, T. L., and Parslow, T. G. (1998) *Nat. Struct. Biol. 5*, 432−436.
18. Mujeeb, A., Parslow, T. G., Zarrinpar, A., Das, C., and James, T. L. (1999) *FEBS Lett. 458*, 387−392.
19. Girard, F., Barbault, F., Gouyette, C., Huynh-Dinh, T., Paoletti, J., and Lancelot, G. (1999) *J. Biomol. Struct. Dyn. 16*, 1145−1157.
20. Theilleux-Delalande, V., Girard, F., Huynh-Dinh, T., and Paoletti, J. (2000) *Eur. J. Biochem. 267*, 2711−2719.
21. Ennifar, E., Yusupov, M., Walter, P., Marquet, R., Ehresmann, B., Ehresmann, C., and Dumas, P. (1999) *Struct. Folding Des. 7*, 1439−1449.
22. Ennifar, E., Walter, P., Ehresmann, B., Ehresmann, C., and Dumas, P. (2001) *Nat. Struct. Biol. 8*, 1064−1068.
23. Jossinet, F., Paillart, J.-C., Westhof, E., Hermann, T., Skripkin, E., Lodmell, J. S., Ehresmann, C., Ehresmann, B., and Marquet, R. (1999) *RNA 5*, 1222−1234.
24. Lodmell, J. S., Ehresmann, C., Ehresmann, B., and Marquet, R. (2000) *RNA 6*, 1267−1276.
25. Lodmell, J. S., Ehresmann, C., Ehresmann, B., and Marquet, R. (2001) *J. Mol. Biol. 311*, 475−490.
26. Takahashi, K.-I., Baba, S., Chattopadhyay, P., Koyanagi, Y., Yamamoto, N., Takaku, H., and Kawai, G. (2000) *RNA 6*, 96−102.
27. Laughrea, M., and Jette, L. (1996) *Biochemistry 35*, 9366−9374.
28. Das, A. T., Klaver, B., Klasens, B. I. F., van Wamel, J. L. B., and Berkhout, B. (1997) *J. Virol. 71*, 2346−2356.
29. Berkhout, B., and van Wamel, J. L. B. (1996) *J. Virol. 70*, 6723−6732.
30. Zuker, M. (1989) *Science 244*, 48−52.
31. Zuker, M., and Turner, D. H. (1999) in *RNA biochemistry and biotechnology* (Barciszewski, J., and Clark, B. F. C., Eds.) pp 11−43, Kluwer Academic Publishers, Dordrecht, Boston, and London.
32. Mathews, D. H., Sabina, J., Zuker, M., and Turner, D. H. (1999) *J. Mol. Biol. 288*, 911−940.
33. Marquet, R., Baudin, F., Gabus, C., Darlix, J. L., Mougel, M., Ehresmann, C., and Ehresmann, B. (1991) *Nucleic Acids Res. 19*, 2349−2357.
34. Muriaux, D., De Rocquigny, H., Roques, B., and Paoletti, J. (1996) *J. Biol. Chem. 271*, 33686−33692.
35. Laughrea, M., Jette, L., Mak, J., Kleiman, L., Liang, C., and Wainberg, M. A. (1997) *J. Virol. 71*, 3397−3406.
36. Berkhout, B., Ooms, M., Beerens, N., Huthoff, H., Southern, E., and Verhoef, K. (2002) *J. Biol. Chem. 277*, 19967−19975.
37. Shen, N., Jette, L., Liang, C., Wainberg, M. A., and Laughrea, M. (2000) *J. Virol. 74*, 5729−5735.
38. Laughrea, M., Shen, N., Darlix, J.-L., Kleiman, L., and Wainberg, M. A. (2001) *Virology 281*, 109−116.
39. Laughrea, M., Shen, N., Jette, L., and Wainberg, M. A. (1999) *Biochemistry 38*, 226−234.
40. Clever, J. L., and Parslow, T. G. (1997) *J. Virol. 71*, 3407−3414.
41. Paillart, J.-C., Berthoux, L., Ottmann, M., Darlix, J.-L., Marquet, R., Ehresmann, B., and Ehresmann, C. (1996) *J. Virol. 70*, 8348−8354.
42. Shen, N., Jette, L., Wainberg, M. A., and Laughrea, M. (2001) *J. Virol. 75*, 10543−10549.
43. Sakuragi, J.-I., Shioda, T., and Panganiban, A. T. (2001) *J. Virol. 75*, 2557−2565.
44. Sakuragi, J.-i., Iwamoto, A., and Shioda, T. (2002) *J. Virol. 76*, 959−967.
45. Dirac, A. M., Huthoff, H., Kjems, J., and Berkhout, B. (2002) *Nucleic Acids Res. 30*, 2647−2655.
46. Poot, R. A., Tsavera, N. V., Boni, I. V., and van Duin, J. (1997) *J. Mol. Biol. 265*, 372−384.
47. Moller-Jensen, J., Franch, T., and Gerdes, K. (2001) *J. Biol. Chem. 276*, 35707−35713.
48. Nocker, A., Hausherr, T., Balsiger, S., Krstulovic, N. P., Hennecke, H., and Narberhaus, F. (2001) *Nucleic Acids Res. 29*, 4800−4807.
49. Schlax, P. J., Xavier, K. A., Gluick, T. C., and Draper, D. E. (2001) *J. Biol. Chem. 276*, 38494−38501.
50. Lease, R. A., and Belfort, M. (2000) *Proc. Natl. Acad. Sci. U.S.A. 97*, 9919−9924.
51. Beck, J., and Nassal, M. (1998) *Mol. Cell. Biol. 18*, 6265−6272.
52. Olsthoorn, R. C. L., Mertens, S., Brederode, F. T., and Bol, J. F. (1999) *EMBO J. 18*, 4856−4864.
53. Hemmings-Mieszczak, M., Steger, G., and Hohn, T. (1997) *J. Mol. Biol. 267*, 1075−1088.

BI025993N